AJNR

Differential Chemosensitivity of Tumor Components in a Malignant Oligodendroglioma: Assessment with Diffusion-Weighted, Perfusion-Weighted, and Serial Volumetric MR Imaging

Hans Rolf Jäger, Adam D Waldman, Christopher Benton, Nicholas Fox and Jeremy Rees

AJNR Am J Neuroradiol 2005, 26 (2) 274-278
http://www.ajnr.org/content/26/2/274

AJNR Am J Neuroradiol 26:274–278, February 2005

Case Report

Differential Chemosensitivity of Tumor Components in a Malignant Oligodendroglioma: Assessment with Diffusion-Weighted, Perfusion-Weighted, and Serial Volumetric MR Imaging

Hans Rolf Jäger, Adam D Waldman, Christopher Benton, Nicholas Fox, and Jeremy Rees

Summary: We report the case of malignant oligodendroglioma in a 36-year-old man who underwent diffusion-weighted, perfusion-weighted, and volumetric MR imaging before and after PCV (procarbazine, CCNU, vincristine) chemotherapy. The tumor regions exhibiting a low apparent diffusion coefficient and increased relative cerebral blood volume showed a marked response to chemotherapy and dramatic decrease in volume, whereas the remaining tumor regions showed little change. Diffusion-weighted and perfusion-weighted MR imaging may be helpful in predicting chemosensitivity of glial tumors.

The realization that certain primary brain tumors are chemosensitive has changed our therapeutic approach, particularly with respect to anaplastic or aggressive oligodendrogliomas. Although uncommon—comprising only 5–10% of adult CNS gliomas—they have a number of clinical and biological features that make them particularly worthy of study. Accurate diagnosis of oligodendrogliomas is now an important issue in clinical neuro-oncology, because overall survival rate and response to treatment may be substantially better than those of other gliomas. Recently, allelic loss of chromosomes 1p and 19q has been identified as an important molecular marker of chemostensitivity (1).

Advanced MR imaging methods such as MR diffusion and MR perfusion provide information about physiological parameters of brain tumors not available with conventional MR images. This additional information can be used to increase the sensitivity of MR imaging in predicting the histologic tumor grade (2, 3).

Case Report

A 36-year-old man presented with a nocturnal generalized seizure. MR imaging showed a T2-hyperintense mass lesion in the right cerebral hemisphere involving the frontal and temporal lobes and insula. Surgical biopsy revealed a low-grade oligodendroglioma. The biopsy was complicated by hemorrhage, from which the patient recovered. Because the histologic findings revealed a low tumor grade and the patient was clinically well and seizure-free, a policy of observation was instituted. Serial MR imaging studies over the next 5 years showed no change in size of the tumor. Subsequently, a small area of subtle, pathologic contrast enhancement appeared in the insular region on an MR image; on this occasion, however, a double dose of gadolinium (2 mmol/kg meglumine gadoterate) had been given, whereas previous studies had used a single dose. Because the patient was clinically well and the tumor had not changed in size, it was decided to await events rather than treat.

Follow-up MR imaging study 6 months later (Fig 1), which included diffusion- and perfusion-weighted and volumetric MR images, showed that the tumor had grown considerably, with the development of mass effect resulting in medial displacement of the basal ganglia, compression of the right lateral ventricle, and midline shift. The posterior and superior portions of the tumor, which involved mostly the right insula, contained areas of cystic degeneration and pathologic contrast enhancement. Apparent diffusion coefficient (ADC) maps showed restricted diffusion with a mean ADC of 0.76×10^{-3} mm^2/s in the solid tumor portion surrounding the complex cyst in the insula. The temporal tumor portion had a mean ADC of 1.44×10^{-3} mm^2/s. The mean ADC measurements of the insular and temporal tumor portions, respectively, corresponded to 93% and 178% of the contralateral normal white matter ADC. MR perfusion imaging showed a large area of increased relative cerebral blood volume (rCBV) in the insular tumor component, with a mean rCBV of 5.49 (ratio to rCBV of contralateral white matter). In contrast, the rCBV of the temporal tumor component was close to that of normal white matter. The areas with decreased ADC and with increased rCBV were both larger than the area of pathologic enhancement on the postcontrast T1-weighted images. At the time of this MR imaging study, the patient had developed a left hemiparesis. He declined a further biopsy and was treated with four cycles of PCV (procarbazine, CCNU, vincristine) chemotherapy. He noticed an improvement within a

Received February 12, 2004; accepted after revision June 14.

From the Institute of Neurology (H.R.J., A.D.W., C.B., N.F., J.R.); Lysholm Department of Neuroradiology, National Hospital for Neurology and Neurosurgery (H.R.J.); and Department of Imaging, Charing Cross Hospital (A.D.W.), London, United Kingdom.

Address correspondence to Hans Rolf Jäger, Lysholm Department of Neuroradiology, National Hospital for Neurology and Neurosurgery, Queen Square, London, United Kingdom WC1N 3BG.

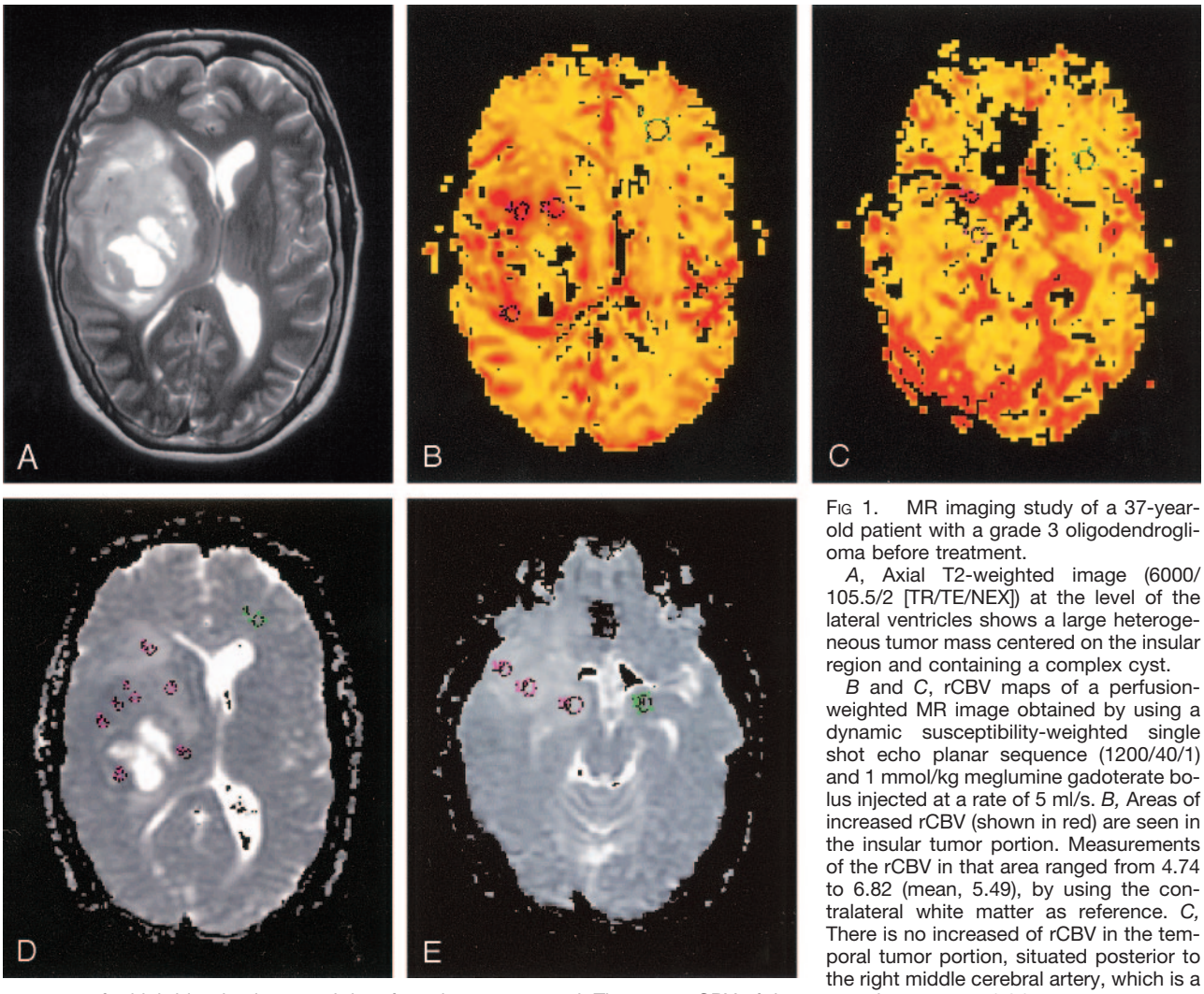

FIG 1. MR imaging study of a 37-year-old patient with a grade 3 oligodendroglioma before treatment.

A, Axial T2-weighted image (6000/105.5/2 [TR/TE/NEX]) at the level of the lateral ventricles shows a large heterogeneous tumor mass centered on the insular region and containing a complex cyst.

B and *C*, rCBV maps of a perfusion-weighted MR image obtained by using a dynamic susceptibility-weighted single shot echo planar sequence (1200/40/1) and 1 mmol/kg meglumine gadoterate bolus injected at a rate of 5 ml/s. *B,* Areas of increased rCBV (shown in red) are seen in the insular tumor portion. Measurements of the rCBV in that area ranged from 4.74 to 6.82 (mean, 5.49), by using the contralateral white matter as reference. *C,* There is no increased of rCBV in the temporal tumor portion, situated posterior to the right middle cerebral artery, which is a structure of a high blood volume and therefore shows up as red. The mean rCBV of the temporal tumor was 1.04.

D and *E*, ADC maps of a diffusion-weighted image (10,000/93.3 [TR/TE]; b = 1,000 s/mm^2). *D*, Axial section at the level of the lateral ventricles shows that the tumor surrounding the complex cyst in right insular region appears hypointense relative to normal white matter. Regions of interest placed in this area had ADC measurements from 0.70 to 0.89 $\times$ 10^{-3} mm^2/s (mean, 0.76) *E*, Axial section through the temporal lobes shows that the tumor in the right temporal lobe appears hyperintense relative to normal white matter, with ADC measurements ranging from 1.39 to 1.49 $\times$ 10^{-3} mm^2/s (mean 1.44).

few days of the first cycle and completely recovered function down the left side by the end of the second cycle. A further MR imaging study, including perfusion- and diffusion-weighted and volumetric sequences, was performed after the fourth chemotherapy cycle (Fig 2). This showed a dramatic reduction of the posterior and superior tumor components that had exhibited low ADC and high rCBV measurements on the initial image. There was near-complete resolution of the complex cyst and normalization of the rCBV. The mean ADC of the small residual insular tumor was now 1.30 $\times$ 10^{-3} mm^2/s. There remained, however, a small area of enhancement.

In contrast, the temporal tumor component showed no significant change in volume, signal intensity characteristics, ADC, or rCBV. We obtained an objective confirmation of the regional differences in tumor volume change following chemotherapy with difference images of the coregistered T1-weighted volumetric images, on which areas of tumor shrinkage are shown in green and areas of CSF expansion in red (Fig 3).

Discussion

Advanced MR imaging techniques are increasingly used as an adjunct to conventional MR imaging in the investigation of cerebral mass lesions, including gliomas. Visual inspection of diffusion-weighted trace images provides little additional information and is hampered by T2-dependent effects; however, measurement of the ADC, which is independent of T2 effects, is a potentially useful method to distinguish between high- and low-grade gliomas (3–6). Water diffusion appears to be more restricted in high-grade gliomas than in low-grade gliomas, resulting in significantly lower ADC values in high-grade tumors. Ranges of ADC measurements in high-grade gliomas reported in different series (expressed as $\times 10^{-3}$

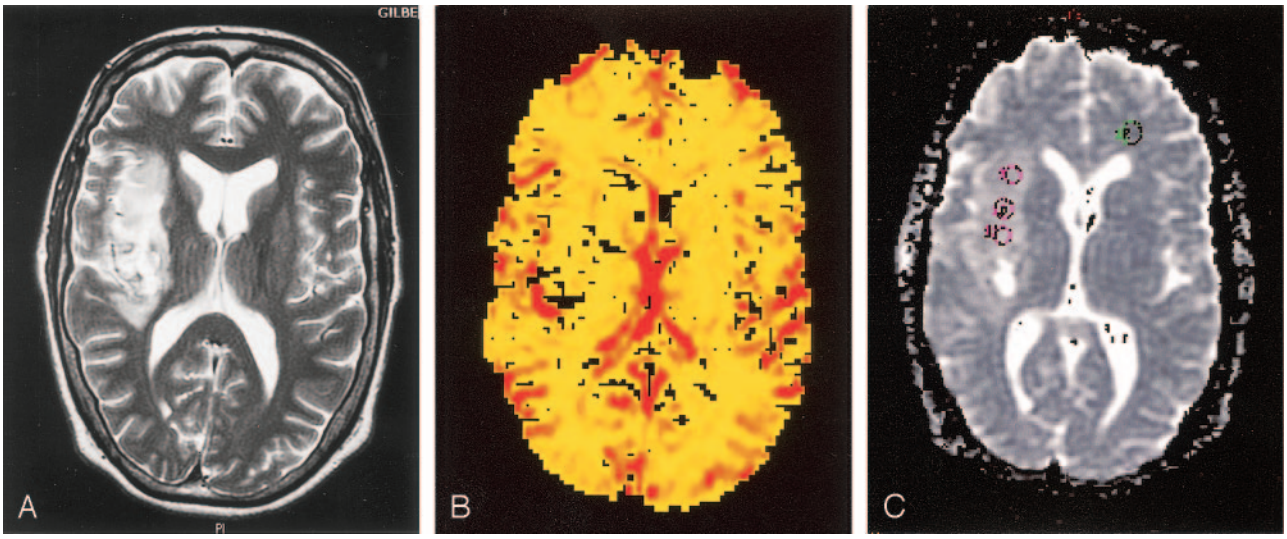

FIG 2. MR imaging study following four cycles of chemotherapy with PCV.

A, Axial T2-weighted image (6000/105.5/2 [TR/TE/NEX]) at the level of the lateral ventricles shows a marked reduction of the insular tumor component with almost complete resolution of the complex cyst.

B, rCBV map of an axial dynamic susceptibility-weighted single shot echo planar sequence (1200/40/1 [TR/TE/NEX]) no longer show any areas of increased rCBV in the residual insular tumor.

C, ADC map of an axial diffusion-weighted image (10,000/93.3 [TR/TE]; b = 1000 s/mm^2) at the level of the lateral ventricles shows that the small residual tumor in the insula is no longer hypointense but hyperintense compared with contralateral white matter, with ADC measurements ranging from 1.21 to 1.38 $\times$ 10^{-3} mm^2/s (mean, 1.30).

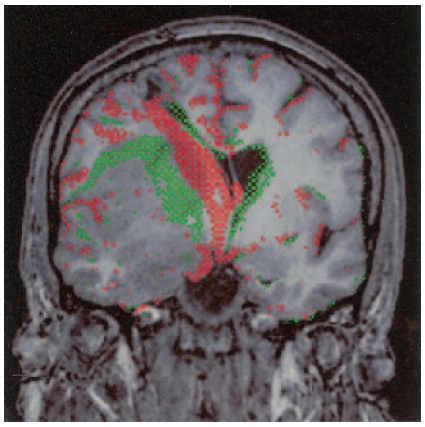

FIG 3. Difference image of volumetric pre- and post-treatment studies. Red-green difference image of pre- and post-treatment coregistered nonenhanced T1-weighted volumetric images (14.4/ 6.4/1[TR/TE/NEX]) with a section thickness of 1 mm. *Green* indicates a shift from lower to higher signal intensity between the first and second study; *red*, the reverse. Reduction in size of the superior (mostly insular) tumor component is shown in *green*, which indicates replacement of T1-hypointense tumor by tissue of higher signal intensity. Re-expansion of the hypointense CSF spaces because of a decrease in mass effect is indicated in *red* (this includes a track leading down to the right lateral ventricle, which is related to a previous biopsy). Note the absence of boundary shifts of the temporal tumor component between the pre- and post-treatment studies.

mm^2/s) were 0.65–1.06, mean 0.82 $\pm$ 0.13 (3); 0.82–2.46, mean 1.2 $\pm$ 0.4 (4); 0.51–1.55, mean 0.92 $\pm$ 0.27 (5); and 0.62–1.29, mean 0.93 $\pm$ 0.19 (6).

Sugahara et al (4) demonstrated a statistically significant inverse relationship between the histologic cell count of gliomas and their ADC measurement, but not with T2 measurements. They postulated that the decreased ADC measurements of high-grade gliomas are primarily due to the increased density of cell nuclei in these tumors, leading to restricted diffusion of water molecules. A recent study (6) showed, however, that the composition of the extracellular tumor matrix, which forms a substantial part of the tumor volume, also influences the ADC measurement. Low-grade tumors contain a greater proportion of hydrophylic components such as hyaluran in their extracellular matrix, which also contributes to an increase in ADC. Malignant oligodendrogliomas frequently appear as inhomogeneous tumors.

In the case reported here, we demonstrated marked differences of regional variation in ADC measurements within the tumor before chemotherapy. The solid portion surrounding the cystic necrotic area in the insular region had markedly lower ADC measurements (range, 0.70–0.89 $\times$ 10^{-3} mm^2/s) than the temporal portion. On the basis of the above-cited study results, it appears likely that the areas with reduced ADC are indicative of regions that have undergone malignant transformation.

These were the areas that happened to respond well to chemotherapy, which led not only to a dramatic regional tumor shrinkage, but also to a significant increase of regional ADC. Following four cycles of chemotherapy, the lowest measured tumor ADC was 1.21 $\times$ 10^{-3} mm^2/s compared with 0.70 $\times$ 10^{-3} mm^2/s before chemotherapy. This corresponds to previously described changes following gene therapy in animal experiments. Stegman et al (7) observed a 31% increase in ADC of gliomas in rats within 8 days of cytosine deaminase gene therapy, preceding changes in tumor growth kinetics and tumor regression. As far as we are aware, there are no previous

reports of measuring ADC changes as an indicator of therapeutic response in humans.

In the reported case, we found markedly increased rCBV measurements (up to 6.82) in the insular tumor portion but not in the temporal region. The area of increased rCBV overlapped with the region of decreased ADC and both were more extensive than the region of pathologic enhancement. Formation of new blood vessels (angiogenesis) represents an important aspect of tumor progression and growth. Microvascular density in glial tumors correlates with histologic tumor grade, and MR perfusion imaging is a noninvasive method of assessing the tumor microvasculature. Sugahara et al (8) were able to show that rCBV measurements correlate closely with angiographic and histologic measures of tumor vascularity. The rCBV measurements of tumors are usually expressed as a ratio with the rCBV of the normal contralateral white matter, because absolute quantification of perfusion parameters with MR imaging is still unreliable. Several studies have shown statistically significant differences of the maximum rCBV (regional rCBV over the most vascular portion of the tumor) in high- and low-grade gliomas. Sugahara et al (8) found mean maximum rCBV values of 7.32, 5.84, and 1.26 for glioblastomas, anaplastic astrocytomas and low-grade gliomas, respectively, which correlate closely with the findings of Yang et al (5), who found mean maximum rCBV values of 6.10 for high-grade gliomas and 1.74 for low-grade gliomas. Law et al (9) recently reported a large study examining the sensitivity, specificity, and predictive values of perfusion-weighted MR imaging in predicting the histologic grade of 160 primary cerebral gliomas. They found that rCBV measurements significantly increased the sensitivity and positive predictive value (PPV) of conventional MR imaging. By using rCBV thresholds of 1.75, MR perfusion imaging had a sensitivity of 95% and PPV of 87%.

In the reported case, the findings at MR perfusion imaging changed significantly after four cycles of chemotherapy. There was no longer any pathologic increase of rCBV within the tumor, whereas a small area of pathologic enhancement persisted on the T1-weighted images, which indicates disruption of the blood-brain barrier.

Regression of rCBV at MR perfusion imaging has previously been described following antiangiogenic therapy of high-grade gliomas, but not after PCV chemotherapy of oligodendrogliomas. Cha et al (10) described 18 patients with recurrent malignant gliomas receiving a combination of thalidomide as an antiangiogenic drug and carboplatin. They found a decline of the rCBV from an average of 6.55 at baseline to 3.40 at 2 months after antiangiogenic therapy. A control group receiving carboplatin alone showed no significant change in rCBV in their study, which included mostly patients with glioblastoma multiforme and a single patient with an oligoastrocytoma in each group. They also found that rCBV measurements correlated better with the clinical status than those of conventional MR imaging.

We acquired volumetric T1-weighted MR images before and after treatment and co-registered these images by using MIDAS image analysis software (11), which permits objective measurement of cerebral volume changes of approximately 0.2% of whole brain volume. There is extensive experience with this technique in the assessment of regional brain volume changes in patients with Alzheimer disease (11), but to our knowledge, this is the first time it has been applied to monitor the therapeutic response of a brain tumor. The dramatic tumor reduction in the insular region is obvious on visual inspection but more objectively shown on the red-green difference images of the coregistered volumetric studies, which confirm also that there has been no subtle volume change in the temporal region. In addition, this technique has revealed changes in the contralateral hemisphere because of reduction of mass effect resulting in opening up of the central sulci.

This is the first report correlating regional differences in chemosensitivity of a malignant oligodendroglioma with diffusion and perfusion MR imaging. Tumor heterogeneity within glial tumors is well documented. It represents a potential source of sampling error during surgical biopsy, which may result in erroneous tumor grading. It has been suggested that MR perfusion imaging might be useful in guiding surgical tumor biopsy (2), because it has the potential to pinpoint areas of malignant transformation with a greater accuracy than conventional MR imaging.

We have been able to demonstrate that perfusion- and diffusion-weighted MR imaging may also be useful for predicting which components of the tumor are likely to respond to chemotherapy and how much tumor shrinkage can be expected. This case report demonstrates that regions showing diffusion and perfusion characteristics of high-grade tumors appear to be more chemosensitive than tumor components exhibiting imaging characteristics of low-grade tumors.

As neoadjuvant chemotherapy of malignant oligodendrogliomas is now discussed as an alternative first-line treatment to radiation therapy (1), these advanced MR imaging methods could be potentially useful in predicting treatment response. The initial findings reported here will need to be corroborated in a larger prospective study. Such a study could also address the question of whether oligodendrogliomas with allelic losses of chromosome 1p and 19q, which are known to be highly chemosensitive, show differences in microvasculature and water diffusion.

References

1. Behin A, Hoang-Xuan K, Carpetier AF, Delattre JY. **Primary brain tumours in adults.** *Lancet* 2003;361:323–331
2. Cha S, Knopp EA, Johnson G, et al. **Intracranial mass lesions: dynamic contrast- enhanced susceptibility-weighted echo- planar perfusion MR imaging.** *Radiology* 2002;223:11–29

3. Kono K, Inoue Y, Nakayama K, et al. **The role of diffusion-weighted imaging in patients with brain tumors.** *AJNR Am J Neuroradiol* 2001;22:1081–1088
4. Sugahara T, Korogi Y, Kochi M, et al. **Usefullness of diffusion-weighted MRI with echo- planar technique in the evaluation of cellularity in gliomas.** *J Magn Reson Imaging* 1999;9:53–60
5. Yang D, Korogi T, Sugahara T, et al. **Cerebral gliomas: prospective comparison of multivoxel 2D chemical-shift imaging proton MR spectroscopy, echoplanar perfusion and diffusion- weighted MRI.** *Neuroradiol* 2002;44:656–666
6. Sadeghi N, Camby I, Goldman S, et al. **Effect of hydrophilic components of the extracellular matrix on quantifiable diffusion-weighted imaging of human gliomas: preliminary results of correlating apparent diffusion coefficient values and hyaluronan expression level.** *AJR Am J Roentgenol* 2003;181:235–241
7. Stegman LD, Rehemtulla A, Hamstra DA, et al. **Diffusion MRI detects early events in the response of a glioma model to the yeast cytosine deaminase gene therapy strategy.** *Gene Ther* 2000;7:1005–1010
8. Sugahara T, Koroghi Y, Kochi M, et al. **Correlation of MR imaging-determined cerebral blood maps with histologic and angiographic determination of vascularity of gliomas.** *AJR Am J Roentgenol* 1998;171:1479–1486
9. Law M, Yang S, Wang H, et al. **Glioma grading: sensitivity, specificity, and predictive values of perfusion MR imaging and proton MR spectroscopic imaging compared with conventional MR imaging.** *AJNR Am J Neuroradiol* 2003;24:1989–1998
10. Cha S, Knopp EA, Johnson G, et al. **Dynamic contrast-enhanced T2-weighted MR imaging of recurrent malignant gliomas treated with thalidomide and carboplatin.** *AJNR Am J Neuroradiol* 2000;21:881–890
11. Freeborough P, Woods R, Fox N. **Accurate registration of serial 3D MR brain images and its application to visualizing change in neurodegenerative disorders.** *J Comput Assist Tomogr* 1996;20:1012–1022